Predicting transient dynamics in a model of reed musical instrument with slowly time-varying control parameter

Baptiste Bergeot, Soizic Terrien, Christophe Vergez

Predicting transient dynamics in a model of reed musical instrument with slowly time-varying control parameter

B. Bergeot,[1] S. Terrien,[2] and C. Vergez[3]
[1)] *INSA CVL, Univ. Orléans, Univ. Tours, LaMé UR 7494, F-41034, 3 Rue de la Chocolaterie, CS 23410, 41034 Blois Cedex, France*
[2)] *Laboratoire d'Acoustique de l'Université du Mans (LAUM), UMR 6613, Institut d'Acoustique - Graduate School (IA-GS), CNRS, Le Mans Université Le Mans, France*
[3)] *Aix Marseille Univ, CNRS, Centrale Med, LMA UMR 7031, Marseille, France*

(*Electronic mail: baptiste.bergeot@insa-cvl.fr)

(*Electronic mail: soizic.terrien@univ-lemans.fr)

(*Electronic mail: vergez@lma.cnrs-mrs.fr)

(Dated: 27 July 2024)

When playing a self-sustained reed instrument (such as the clarinet), initial acoustical transients (at the beginning of a note) are known to be of crucial importance. Nevertheless, they have been mostly overlooked in the literature on musical instruments. We investigate here the dynamic behavior of a simple model of reed instrument with a time-varying blowing pressure accounting for attack transients performed by the musician. In practice, this means studying a one-dimensional non-autonomous dynamical system obtained by slowly varying in time the bifurcation parameter (the blowing pressure) of the corresponding autonomous systems, i.e., whose bifurcation parameter is constant. In this context, the study focuses on the case for which the time-varying blowing pressure crosses the bistability domain (with the coexistence of a periodic solution and an equilibrium) of the corresponding autonomous model. Considering the time-varying blowing pressure as a new (slow) state variable, the considered non-autonomous one-dimensional system becomes an autonomous two-dimensional fast-slow system. In the bistability domain, the latter has attracting manifolds associated with two stable branches of the bifurcation diagram of the system with constant parameter. In the framework of the geometric singular perturbation theory, we show that a single solution of the two-dimensional fast-slow system can be used to describe the global system behavior. Indeed, this allows to determine, depending on initial conditions and rate of change of the blowing pressure, which manifold is approached when the bistability domain is crossed and to predict whether a sound is produced during transient as a function of the musician's control.

As many dynamical systems, musical instruments have been shown to sustain a possibly high degree of multistability, corresponding to the coexistence of stable solutions (equilibria, periodic and quasiperiodic solutions as well as chaotic regimes) for a given set of parameters. In the simple model of reed musical instrument considered here, multistability manifests itself by the coexistence of a periodic solution (i.e., a musical note) and an equilibrium (i.e., the silence) in a region of the bifurcation diagram referred to as bistability domain. In this context, we investigate the behavior of this simple reed instrument model when the blowing pressure (the main control parameter in practice) is varied over time and crosses the bistability domain of the corresponding model with constant parameter. This is motivated by the will of achieving a better understanding of the role of attack transients performed by the musician on the behavior of actual instruments, including their transient dynamics. Indeed, because such instruments have a very rich dynamics with respect to the blowing pressure, many different regions with qualitatively different and possibly multistable dynamics are likely to be crossed during the attack of a note. In our simple model, when the bistability domain is crossed, the system can remain close to its current position and follow an attracting invariant manifold (no sound is produced during attack transient), or leave it abruptly to reach the other attracting invariant manifold (a sound is produced during attack transient). We show that this depends on the characteristics of the time-varying parameter and we predict whether or not a sound is produced during the attack transient. More precisely, considering the framework of the geometric singular perturbation theory (GSPT), we define and compute a particular trajectory which splits the phase space into two subsets. This allows us to know which initial conditions cause one or the other of these two attracting manifolds to be followed while crossing the bistability domain and as such to predict whether or not a sound is produced during the attack transient.

I. INTRODUCTION

Self-sustained musical instruments such as wind instruments, bowed string instruments or the singing voice are dynamical systems known to produce a wide diversity of regimes. This includes a number of equilibrium and periodic solutions as well as quasiperiodic and chaotic regimes[17,20,29,35,52]. In a musical context, equilibria correspond to silence and periodic solutions are, most often, the desired regimes. They correspond to musical notes with different acoustical features. In particular, fundamental frequency and frequency content (Fourier spectrum) of the periodic solution are associated to the pitch and timbre of a note, respec-

tively. As many dynamical systems in a range of applications, musical instruments have been shown to sustain a possibly high degree of multistability.

An important specificity of self-sustained instruments is that their operation (namely sound production in a musical context) is associated to time-varying control parameters which are adjusted continuously by the musician. For example, wind instruments players control finely and continuously the air pressure in their mouth to obtain the desired sound regime. In particular, attack transients, which correspond to the transient dynamics of the blowing pressure from its initial value (corresponding either to a zero overpressure in the musician's mouth or to the blowing pressure used to play a previous note) to its target value, selected by the musician to play the desired sound regime, have been shown to be of particular importance[21,46]. Indeed, they determine initial acoustical transients, i.e. the beginning of the sound, which are known to be crucial for both sound production and sound perception[48]. In the literature, comparisons between beginners and experienced musicians suggest that some characteristics of attack transients relate to physiological constraints, but also showed that experienced musicians control different aspects of these attack transients to reach the desired sound regime in a reliable manner[21,46] . In particular, experimental observations[22] have shown that control parameters evolve on a slower timescale than acoustical variables related to the instrument internal dynamics. Despite their importance, time-varying control parameters in general and attack transients in particular have been mostly overlooked in the literature on nonlinear dynamics of self-sustained musical instruments. In physical models in particular, control parameters are generally assumed to be constant. Few studies investigated experimentally and numerically the dynamics of a clarinet with slowly varying blowing pressure, with a focus on the effect of both noise and the rate of change of the control parameter. Previous theoretical works by the authors[7,8,10] investigated the emergence of oscillations in simple models of reed instruments when the blowing pressure varies over time. This allowed to interpret experimental results[9] as the manifestation of the bifurcation delay phenomenon. Nevertheless, the timescales considered for the blowing pressure were even slower than those of experimentally-observed attack transients. More recently, Colinot *et al.* showed that, in a multistable physical model of single-reed instrument, different attack transients can lead to different sound regimes being observed in the long term, after any transient dynamics has died out[18]. Overall, to the best of the authors knowledge, the influence of time-varying control parameters on the acoustical transient of the instrument has not been investigated theoretically.

From a more general point of view, nonlinear dynamics of multistable systems with time-varying parameters has attracted considerable attention in the last years, see for example[25,47] as an entry point to the literature. Many studies focused on critical transitions, also referred to as tipping points in climate sciences, that correspond to regime shifts due to changing conditions with applications in fields as diverse as physics, neurosciences, climate science, biology and ecology[3,25]. Ashwin *et al.*[3] proposed a classification of critical transitions based on the mathematical description of the underlying mechanisms: noise-induced transitions, where noise makes a multistable system switch between two stable states, bifurcation-induced transitions and rate-induced transitions. Bifurcation-induced tipping occurs when the time-varying parameter crosses a bifurcation point (for example a fold) and also relates to dynamic bifurcation[6]. Rate-induced tipping, identified by Wieczorek *et al.*[55], occurs when the external forcing (or control parameter) evolves with a rate of increase that has exceeded a critical value, usually without crossing any bifurcation point. More precisely, the system can deviate significantly from its evolving stable solutions under the effect of the changing parameter and crosses a threshold as such, for example a boundary between basins of attraction (a phenomenon referred to as basin instability[43]).

In both bifurcation-induced and rate-induced transitions, the difference between the internal timescales of the system and the timescale of the evolving parameters have been shown to play a crucial role[47]. In bifurcation-induced transitions, sufficiently different timescales can result in bifurcation delay[6,11,33,53]. In the case of rate-induced transitions, the timescales difference relates directly to the critical rate of change of the parameter above (or sometimes below) which transitions occur[47]. In particular, in the case of transitions between equilibrium solutions, Ashwin *et al.*[3] derived the critical rate of change above which the system leaves the solution branch it was going along. In Ref. 2, Ashwin *et al.* introduce a formalism that uses so-called pullback attractors to describe the phenomena of bifurcation-induced transitions and rate-induced transitions, again considering equilibria. The method has been extended by Alkhayoun and Ashwin[1] to periodic solutions. Combining compactification technique[57] with concepts from Geometric Singular Perturbation Theory[24] (GSPT), Wieczorek *et al.*[56] developed a mathematical framework for the study of rate-induced tipping for asymptotically autonomous dynamical systems, i.e., with time-varying parameters having finite limits when the time tends to infinity. O'Sullivan *et al.*[45] introduced a complementary framework to analyze rate-induced tipping in a non-autonomous (and also asymptotically autonomous) fast-slow dynamical system. In actual physical systems, critical transitions may be associated with a combination of noise-induced, bifurcation-induced and rate-induced transitions.

Here we consider a state-of-the-art model of reed musical instruments, written as a n-dimensional system of ordinary differential equations, where n relates to the number of acoustical modes taken into account[15] to model the instrument resonator:

$$\dot{x} = f(x, \gamma), \tag{1}$$

with $x \in \mathbb{R}^n$ the vector of state variables (i.e., the modal coordinates of the mouthpiece pressure and their first time derivative) and γ the considered control parameter. The function $f : \mathbb{R}^n \times \mathbb{R} \to \mathbb{R}^n$ is assumed to be sufficiently smooth. In the simple case where a single acoustical mode is considered ($n = 2$) and when a constant blowing pressure is considered, a bifurcation analysis shows that different regions with qualitatively different dynamics are found when the blowing pres-

sure is considered as a bifurcation parameter. For both low and high values of the blowing pressure, an equilibrium corresponding to silence is the only stable solution. In between these two regions, one finds a range of the blowing pressure where a periodic solution corresponding to a musical note is the only stable solution, and a bistability region where the stable periodic solution and the stable equilibrium coexist.

In this article, we consider this model with a time-varying blowing pressure accounting for attack transients performed by the musician, and we focus on the case where the blowing pressure crosses the bistability region (without saturating inside this region): as such, the question of which regime is obtained in the long term is trivial. Rather, we aim at predicting transient dynamics of the system itself (i.e. acoustical transient at the sound onset, which are known for their importance in a musical context), with respect to the characteristics of the control parameter such as its rate of change. This is motivated by practical aspects of instrument playing: when the musician performs an attack transient, the mouth pressure evolves from an initial value which is most often close to zero[22] towards a target value at which the desired sound regime exists and is stable. Because the dynamics of these instruments with respect to the blowing pressure can be rich, the system is likely to cross several regions of the bifurcation diagram with qualitatively different dynamics during the attack transient of the control parameter, thus resulting in possibly complex transient dynamics.

In practice, the model is rewritten as a $(n+1)$-dimensional autonomous system:

$$\dot{x} = f(x,y), \tag{2a}$$
$$\dot{y} = \varepsilon g(y), \tag{2b}$$

associated to Eq. (1) where the control parameter of System (1) varies in time and is written as a new state variable y. The function $g : \mathbb{R} \to \mathbb{R}$ is also assumed to be sufficiently smooth. Eq. (2b) being an autonomous first-order ordinary differential equation its solution $y(t)$ is monotonic, we assume here that it is a monotonically increasing function. Here, ε is a small parameter accounting for the slow evolution of the blowing pressure with respect to the acoustical variables. Overall, system (2) is a slow-fast dynamical system where y is the slow variable and x is the vector of the n fast variables. We adopt a slow-fast dynamical point of view, and consider the framework of GSPT which provides general results on the complicated dynamics of slow-fast dynamical systems by exploiting the separation between the different timescales. In particular here, solutions of (1) are not solutions of (2) since y is not constant in time anymore. Nevertheless, stable solutions of (1) are associated with attracting invariant manifolds of (2)[24,32]. In this context, we focus on the parameter region for which System (1) (with constant control parameter) is bistable. When the control parameter varies in time and crosses this bistability region, we aim at determining the transient dynamics of variables x of System (2) and, in particular, at determining toward which attracting manifold the system is attracted while this region is crossed. In the case mentioned above where an equilibrium solution coexists with a stable periodic solution, this corresponds at determining whether or not the instrument produces a sound during the attack transient. In more complicated (and realistic) cases where a region with several stable periodic solutions is crossed during an attack transient, this means determining which musical note is played during the attack transient. To provide an initial answer to this question, we investigate a simple problem of bistability in which the instrument model with constant control parameter reduces to a one-dimensional nonlinear ODE (i.e., of type (1) with $x \in \mathbb{R}$, it corresponds to the system with $n = 2$ mentioned above which has been reduced by an averaging technique) having, in an interval $D \subset \mathbb{R}$, two coexisting stable equilibria (one corresponds to silence and the other to a musical note[36]). Basins of attraction of these equilibria are separated by an unstable equilibrium. For the same ODE with a control parameter varying slowly in time (i.e., of type (2) with $x \in \mathbb{R}$), for $x \in D$, the stable equilibria become attracting one-dimensional invariant manifolds and the unstable equilibrium becomes a repelling one-dimensional invariant manifold that evolves in the two-dimensional phase space of (2). We find that a given trajectory of (2), denoted as S and whose section for $x \in D$ is the repelling manifold mentioned above, splits the two-dimensional phase space into two subsets. Trajectories resulting from initial conditions in the first subset will follow one of the attracting manifolds when D is crossed, while trajectories resulting from initial conditions in the second subset will follow the other attracting manifold. This represents two qualitatively different behaviors for the system, one corresponds to silence during transient and the other to a musical note played during transient. It is interesting to see that a single object (i.e., S) allows to describe this global (and non trivial) behavior during transients.

The paper is organized as follows. In Section II, the model of single reed instrument under consideration is briefly presented. The bifurcation diagram of the model is computed in Section III. Elements of geometric singular perturbation theory required for the study are recalled in Section IV. Section V presents and illustrates the methodology proposed to predict the nature of the transient behavior of the model. In Section VI, the case where the blowing pressure saturates in the bistability domain is discussed together with the possible extension of the method to more realistic models of instruments. Finally, concluding remarks and some perspectives are given in Section VII.

II. BACKGROUND ON THE PHYSICAL MODEL OF REED INSTRUMENT

The model of single reed instrument model considered in the paper consists in a classical toy model obtained under strong assumptions (see Section A 1). For sake of conciseness, details on the clarinet model (which is classical in musical acoustics) are presented in the Appendix A.

The state variables are the pressure p at the entrance to the instrument resonator (i.e., inside the mouthpiece) and its first time derivative and the bifurcation parameter is the blowing pressure γ (the control parameter under consideration in this work). We consider the averaged dynamics of this model, in

TABLE I. Modal and embouchure parameters. Taken from Ref. 28. Unless stated otherwise, these parameter values are used throughout the article.

Modal parameters	$\varepsilon_1 = 1/36.6$
	$\omega_1 = 1440$
	$Z_1 = 50$
Embouchure parameter	$\zeta = 0.1$

which the amplitude x of p is a state variable, with a time-varying blowing pressure, now considered as another state variable and denoted y (see Section A 2).

Equations of the averaged dynamics are of the form of Eq. (2) where the generic functions f and g are now specific functions defined in Appendix A with now $f : \mathbb{R}^2 \to \mathbb{R}$, i.e.,

$$\dot{x} = f(x,y), \tag{3a}$$
$$\dot{y} = \varepsilon g(y), \tag{3b}$$

with $(x,y) \in \mathbb{R}^2$. Eq. (3a) is the equation of the physical instrument model and Eq. (3b) describes the time variation of the blowing pressure y. The function f is derived from the so-called nonlinear characteristic (NLC) of the instrument exciter which links the volume flow through the reed channel to the pressure difference between the mouth and the mouthpiece and has been widely studied in the literature[19,31].

III. BIFURCATION DIAGRAM OF THE MODEL

Bifurcation analysis is a common method in musical acoustics (see e.g. Refs. 15 and 28). The resulting bifurcation diagrams provides useful information beyond the case with constant control parameters and have shown their interest in the case with slowly time-varying blowing pressure, in particular in simple models of reed musical instruments[7,8,10]. Here, the bifurcation diagram is computed by stating $\dot{y} = 0$ with $y = \text{const.} = \gamma$ in Eq. (3). Fixed points of $\dot{x} = f(x,\gamma)$ (with f given by Eq. (A16)) are computed by solving $f(x,\gamma) = 0$. In practice, we use the function `NSolve` of the Mathematica software[59].

The trivial fixed point is the equilibrium solution of the original (non-averaged) dynamics (A7) and the non trivial fixed points correspond to the two periodic solutions of (A7). The stability of the fixed points is determined subsequently from the sign of $\partial_x f(x,\gamma)$.

Fig. 1 shows the bifurcation diagram obtained for the modal parameters of the air-column and the embouchure parameter ζ given in Table I. Unless stated otherwise, the parameter values given in Table I are used throughout the article. Fig. 1 shows that the model is bistable between $\gamma = 1.11$ and $\gamma = 1.34$. Within this range of the parameter value the trivial fixed point and a non trivial fixed point are stable and, lying between them, the other non trivial fixed point is unstable.

For a given stable solution, the *basin of attraction* (BA) is the set of initial conditions leading to this solution. Here, for our 1D system $\dot{x} = f(x,\gamma)$, the separatrix between the BAs of the two stable fixed points in the bistability domain is trivial, and is the unstable fixed point.

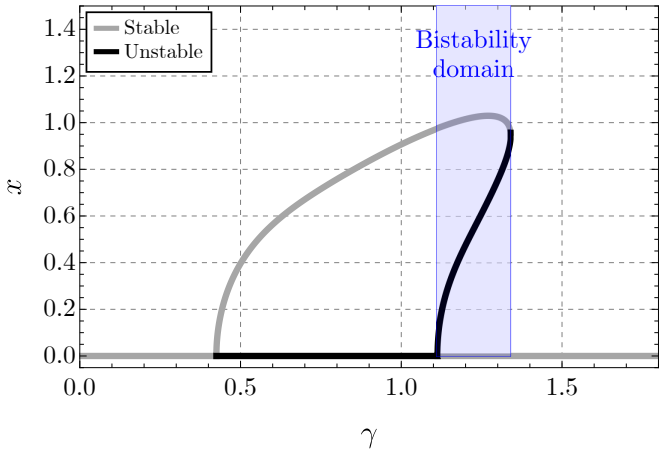

FIG. 1. Bifurcation diagram of the clarinet obtained by averaging procedure. A bistability domain is observed between $\gamma = 1.11$ and $\gamma = 1.34$ and depicted by an blue colored area. The parameters given in Table I are used.

IV. ELEMENTS OF GEOMETRIC SINGULAR PERTURBATION THEORY

In this section some basics of the geometric singular perturbation theory (GSPT)[32] are recalled for the planar dynamical systems called $(1,1)$-fast-slow system, i.e., with one fast state variable and one slow state variable.

System (3), which is obtained as detailed in Appendix A, is considered for sake of illustration. It is a $(1,1)$-fast-slow system where the amplitude x of the mouthpiece pressure is the fast variable and the blowing pressure y is the slow variable.

Eq. (3) is now written on the slow timescale $\tau = \varepsilon t$, Eq. (3) becomes

$$\varepsilon x' = f(x,y) \tag{4a}$$
$$y' = g(y), \tag{4b}$$

where $(x,y) \in \mathbb{R}^2$ and $\{\}' = d_\tau\{\}$ (the first time derivative with respect to the slow time τ).

As an illustration, Fig. 2 shows an example of possible time series $x(\tau)$ and $p(\tau)$ obtained from the numerical integration of the averaged System (4) and of the original System (A7) (replacing γ par $y(t')$ and switching from t' to t, see Appendix A), respectively. We considered a linear time variation of the slow variable, i.e.,

$$y(\tau) = \tau + y_0, \tag{5}$$

or $y(t) = \varepsilon t + y_0$, with $y_0 = y(0)$. Therefore, the function $g(y)$ is simply

$$g(y) = 1. \tag{6}$$

We used the parameters given in Table I.

The time profile of the linearly increasing blowing pressure $y(\tau)$ is also represented. Overall, the figure shows an excellent agreement between time series $x(\tau)$ and $p(\tau)$ which validates the averaging procedure.

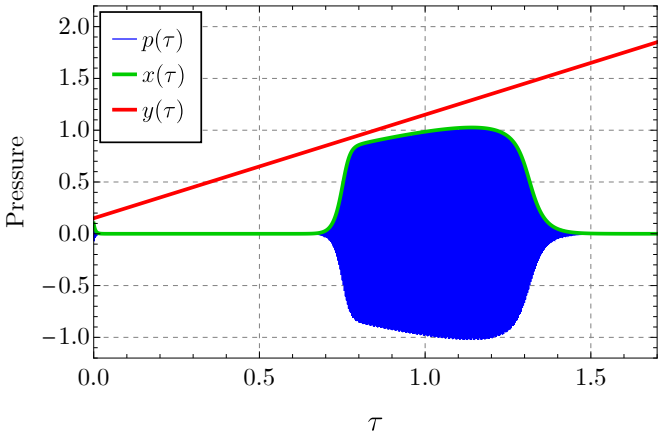

FIG. 2. Times series $x(\tau)$ (green) and $p(\tau)$ (blue) obtained from the numerical integration of the averaged system (4) and of the original System (A7) (replacing γ by $y(t')$ and switching from t' to t, see Appendix A), respectively. Both are obtained with $g(y) = 1$. The time profile of the linearly increased blowing pressure $y(\tau)$ is also represented (red). The parameters given in Table I are used with $\varepsilon = 0.0183$. The initial conditions are: $x(0) = p(0) = 0.1$, $\dot{p}(0) = 0$ and $y(0) = 0.15$.

The time evolution of slow-fast systems is characterized by possible successions of fast epochs and slow epochs. This is shown in Fig. 2. Indeed, the variable x first decreases rapidly to zero (first fast epoch). Then during the increase of the mouth pressure, x follows zero (first slow epoch) and increases rapidly at $\tau \approx 0.65$ (second fast epoch). A slow evolution follows corresponding to oscillations of the mouthpiece pressure p (second slow epoch). Finally, x decreases again rapidly to zero at $\tau \approx 1.45$ (third fast epoch) and follows zero slowly (third slow epoch).

In the GSPT framework, the so-called *slow subsystem* is obtained by stating $\varepsilon = 0$ in Eq. (4), which leads to

$$0 = f(x,y) \tag{7a}$$
$$y' = g(y). \tag{7b}$$

The dynamics of (7) approximates the dynamics of (3) (or (4)) during slow epochs. It is restricted to the *critical manifold* $\mathscr{M}_0$ defined below.

Definition IV.1 (Critical manifold[12])**.** The critical manifold is defined as

$$\mathscr{M}_0 = \left\{(x,y) \in \mathbb{R}^2 \mid x = x^\star(y)\right\} \tag{8}$$

with $x^\star(y)$ the branches of the solution of

$$f(x^\star(y),y) = 0 \tag{9}$$

in each interval of y where $\partial_x f(x,y)$ does not vanish and therefore where we can write that $f(x,y) = 0$ is equivalent to $x = x^\star(y)$ by the *implicit function theorem*.

Note that the critical manifold does not depend on the function $g(y)$.

Points on the critical manifold are equilibria (or fixed points) of the so-called *fast subsystem* defined by

$$\dot{x} = f(x,y) \tag{10a}$$
$$\dot{y} = 0 \tag{10b}$$

which describes the dynamics of the variable x for a constant bifurcation parameter. This corresponds to the static case considered in Section III.

Definition IV.2 (Kuehn[34])**.** Let $a^*(y) : \mathbb{R} \to \mathbb{R}$ be the linearization of the fast vector field (10) on $\mathscr{M}_0$, i.e., at $x = x^\star(y)$, defined as

$$a^\star(y) = \partial_x f\left(x^\star(y),y\right). \tag{11}$$

A value $x^\star(y)$ of the fast variable x is a hyperbolic equilibrium point of (10) if $a^\star(y) \neq 0$; stable if $a^\star(y) < 0$ and unstable if $a^\star(y) > 0$. Then, the critical manifold is called *attracting* (resp. *repelling*) if $a^\star(y) < 0$ (resp. $a^\star(y) > 0$) for $y \in I$ with I a subset of $\mathbb{R}$. A subset $\mathscr{M}_0^{\mathrm{nh}}$ of the critical manifold $\mathscr{M}_0$ is *normally hyperbolic* if for each point $P = (x^\star(y),y) \in \mathscr{M}_0^{\mathrm{nh}}$ we have $a^\star(y) \neq 0$, i.e., $\mathscr{M}_0^{\mathrm{nh}}$ is either attracting or repelling[37].

A simple form of the Fenichel's theorem (from[13]) is given below. It states that all orbits starting near an attracting branch of the critical manifold actually converge to an invariant manifold.

Theorem IV.1 (Fenichel 1979[24], reproduced from Ref. 13)**.** *If the critical manifold $\mathscr{M}_0$ is normally hyperbolic (i.e. attracting or repelling), then there exists a manifold $\mathscr{M}_\varepsilon$, which is $\mathscr{O}(\varepsilon)$-close[38] to $\mathscr{M}_0$ and invariant under the flow (3)[39] (or (4)). The manifold $\mathscr{M}_\varepsilon$ is normally hyperbolic, i.e., it attracts or repels neighboring orbits exponentially fast in directions normal to itself.*

For a more complete statement of the Fenichel's theorem see e.g. Chap. 3 of Ref. 34.

Definition IV.3 (Kuehn[34])**.** The manifold $\mathscr{M}_\varepsilon$, as obtained by the Theorem IV.1, is called the *slow manifold*.

Here and as often, we say "the" manifold $\mathscr{M}_\varepsilon$. Formally, this is incorrect. Indeed, the complete statement of the Fenichel's theorem stipulates that $\mathscr{M}_\varepsilon$ is usually not unique. However, it also stipulates that all these manifolds are exponentially close to each other, i.e., they lie at a distance[38] $\mathscr{O}(e^{-K/\varepsilon})$ from each other for some $K > 0$ with $K = \mathscr{O}(1)$. Consequently, we adopt the convention to refer to $\mathscr{M}_\varepsilon$ as "the" slow manifold of Eq. (4).

V. PREDICTING THE NATURE OF TRANSIENTS

This section presents the main results of this work.

We consider the $(1,1)$-fast-slow system (3) (or (4)) whose critical manifold $\mathscr{M}_0$ (see Definition IV.1) has a bistability domain as depicted here in Fig. 1[40].

The bistability domain of $\mathscr{M}_0$ is the following subset

$$U_D = \mathbb{R} \times D \tag{12}$$

of $\mathbb{R}^2$, with $D=(y_\mathrm{l},y_\mathrm{u})$. The complement U_D is denoted as U_D'. In U_D the critical manifold $\mathscr{M}_0$, defined by Eq. (8), has two attracting branches $x_1^\star(y)$ and $x_2^\star(y)$, i.e., $a_1^\star(y)=\partial_x f(x_1^\star(y),y)<0$ and $a_2^\star(y)=\partial_x f(x_2^\star(y),y)<0$, corresponding to the stable branches of the bifurcation diagram shown in Fig. 1. Necessarily, $\mathscr{M}_0$ has also a repelling branch $x_3^\star(y)$ for which $a_3^\star(y)=\partial_x f(x_3^\star(y),y)>0$ and correspnding to the unstable branch of the bifurcation diagram shown in Fig. 1. The critical manifold is non normally hyperbolic at $y=y_\mathrm{l}$ and $y=y_\mathrm{u}$. For the model of reed instrument studied here with the parameters given in Table I, one has $y_\mathrm{l}=1.11$ and $y_\mathrm{u}=1.34$ (see Fig. 1).

From now on, we will focus on the behavior of the system before and during the crossing of U_D. Consequently, we consider that in Eqs. (3) and (4) one has $(x,y)\in U$ with U the set of $\mathbb{R}^2$ defined as

$$U=\mathbb{R}\times(-\infty,y_\mathrm{u}). \tag{13}$$

In U_D (see Eq. (12)) the critical manifold $\mathscr{M}_0$ of (4) has two coexisting attracting branches $\mathscr{M}_{0,\mathrm{a}_1}$ and $\mathscr{M}_{0,\mathrm{a}_2}$ defined as

$$\mathscr{M}_{0,\mathrm{a}_i}=\{(x,y)\in U_D\mid x=x_i^\star(y)\},\quad i=1,2 \tag{14}$$

separated by a repelling branch $\mathscr{M}_{0,\mathrm{r}}$

$$\mathscr{M}_{0,\mathrm{r}}=\{(x,y)\in U_D\mid x=x_3^\star(y)\}. \tag{15}$$

Through Fenichel's Theorem IV.1, Eq. (4) has two attracting invariant manifolds $\mathscr{M}_{\varepsilon,\mathrm{a}_i}$ $\mathscr{O}(\varepsilon)$-close to $\mathscr{M}_{0,\mathrm{a}_i}$ $(i=1,2)$ and a repelling slow invariant manifold $\mathscr{M}_{\varepsilon,\mathrm{r}}$ $\mathscr{O}(\varepsilon)$-close to $\mathscr{M}_{0,\mathrm{r}}$ defined as

$$\mathscr{M}_{\varepsilon,\mathrm{a}_i}=\{(x,y)\in U_D\mid x=\bar{x}_i(y,\varepsilon)\},\quad i=1,2 \tag{16}$$

with $\bar{x}_i(y,\varepsilon)=x_i^\star(y)+\mathscr{O}(\varepsilon)$, and

$$\mathscr{M}_{\varepsilon,\mathrm{r}}=\{(x,y)\in U_D\mid x=\bar{x}_3(y,\varepsilon)\} \tag{17}$$

with $\bar{x}_3(y,\varepsilon)=x_3^\star(y)+\mathscr{O}(\varepsilon)$. We chose arbitrarily that $\mathscr{M}_{\varepsilon,\mathrm{a}_1}$ is the branch corresponding to $x_1^\star(y)=0$.

Fenichel's theorem states that the branches of $\mathscr{M}_\varepsilon$ are normally hyperbolic (either attracting or repelling) and are $\mathscr{O}(\varepsilon)$-close to $\mathscr{M}_0$ only if $y\in D$. However, the curves $\bar{x}_i(y,\varepsilon)$ $(i=1,2)$ and $\bar{x}_3(y,\varepsilon)$, which are given solutions of Eq. (3) or Eq. (4), continue to exist to the left of D for $y<y_\mathrm{l}$. Moreover, because a solution starting from any point in U is uniquely determined, one knows (if we assume without loss of generality that $\bar{x}_1(y,\varepsilon)<\bar{x}_3(y,\varepsilon))$ $\bar{x}_2(y,\varepsilon)>\bar{x}_3(y,\varepsilon)$ for $y\in D$, that $\bar{x}_1(y,\varepsilon)<\bar{x}_3(y,\varepsilon)$ and $\bar{x}_2(y,\varepsilon)>\bar{x}_3(y,\varepsilon)$ when $y<y_\mathrm{l}$. Consequently, a solution of Eq. (3) or Eq. (4) that starts in a point in U_D' with $x<\bar{x}_3(y,\varepsilon)$ (resp. $x>\bar{x}_3(y,\varepsilon)$) enters the bistability domain with also $x<\bar{x}_3(y,\varepsilon)$ (resp. $x>\bar{x}_3(y,\varepsilon)$) and, since ε is small, will quickly be attracted by $\mathscr{M}_{\varepsilon,\mathrm{a}_1}$ (resp. $\mathscr{M}_{\varepsilon,\mathrm{a}_2}$). Therefore, the solution $\bar{x}_3(y,\varepsilon)$ in the whole domain U, denoted as S and defined as

$$S=\{(x,y)\in U\mid x=\bar{x}_3(y,\varepsilon)\}, \tag{18}$$

splits U into two subsets, denoted as B_i $(i=1,2)$ and defined as

$$B_1=\{(x,y)\in U\mid x<\bar{x}_3(y,\varepsilon)\} \tag{19}$$

and

$$B_2=\{(x,y)\in U\mid x>\bar{x}_3(y,\varepsilon)\}, \tag{20}$$

respectively, with therefore

$$U=B_1\cup S\cup B_2. \tag{21}$$

Note that S follows a repelling manifold along its entire length, therefore through Ref. 54 it can be seen as a *maximum canard* solution of (4).

The solution S therefore provides useful information on the global behavior of the system in U. Indeed, orbits originating from initial conditions in B_i end up following $\mathscr{M}_{\varepsilon,\mathrm{a}_i}$ $(i=1,2)$ when the slow variable y crosses the interval D, this indicates if a sound is played or not during transient (even if this conclusion can be questioned for trajectories initialized very close to S, this is discussed here). Considering that it allows to predict a qualitative change in the system behavior, S relates to the so-called rate-tipping thresholds and quasithresholds. These concepts are rigorously defined in Refs. 56 and 45 for asymptotically autonomous dynamical system, i.e., with a time-varying parameter having a finite limit when the time tends to infinity (which is not the case here), by means of a methodology which combines the compactification technique[57] with concepts from GSPT[24].

The question of whether a given trajectory will reach $\mathscr{M}_{\varepsilon,\mathrm{a}_1}$ or $\mathscr{M}_{\varepsilon,\mathrm{a}_2}$ is relatively simple if the initial condition of the trajectory is in U_D since the Fenichel's theorem guarantees that $\bar{x}_3(y,\varepsilon)=x_3^\star(y)+\mathscr{O}(\varepsilon)$. Moreover, asymptotic analytical expressions of $\bar{x}_3(y,\varepsilon)$, in the form of a power series in ε, can be easily obtained for $y\in D$ (see e.g. Ref. 13). These approximations fail in the vicinity of non hyperbolic points[41], especially here at $y=y_\mathrm{l}$.

In the study of bifurcation-induced and rate-induced transitions (and especially in a musical context when the musician starts a note) it is more crucial to know which attracting branch $\mathscr{M}_{\varepsilon,\mathrm{a}_i}$ ($i=1$ or 2) will be reached for an initial condition in U_D'. In this case, the problem is no longer simple because along S non-hyperbolic points are approached in which the scaling laws (see Note 40) are not easy to obtain in general and where bifurcation delay can appear.

Because analytical methods based on finding scaling laws seem very complicated to generalize to higher dimensional systems we focus on numerical methods. As a canard solution, S is very sensitive to parameter variations and it is therefore hard to detect using numerical direct time integration. The general idea is here to first determine S in U_D (in which Fenichel's theorem guarantees that it is normally hyperbolic and $\mathscr{O}(\varepsilon)$-close to the critical manifold) and subsequently deduce S in U_D' to finally obtain S in U. Because S is repelling in U_D, in the manner of Berglund and Landon[14], the simplest way to compute S is here a time reversal numerical integration starting in U_D close to the critical manifold. Note that in higher dimensional systems, in which the solutions equivalent to S will probably be locally saddle-type manifolds (i.e., associated with both negative and positive eigenvalues of the fast subsystem), advanced numerical methods (e.g. continuations methods) must be used (see the discussion in Section VI B).

Then, S is here approximated by the numerical integration of

$$\varepsilon x' = -f(x,y) \tag{22a}$$
$$y' = -g(x,y) \tag{22b}$$

choosing an initial condition (x_0, y_0) on the upper boundary of the bistability domain D and on the repelling part $\mathscr{M}_{0,\mathrm{r}}$ of the critical manifold, i.e.,

$$(x_0, y_0) = (x_3^\star(y_\mathrm{u}), y_\mathrm{u}). \tag{23}$$

We use the fact that, through Theorem IV.1, $\mathscr{M}_{0,\mathrm{r}}$ is $\mathscr{O}(\varepsilon)$-close to the corresponding repelling invariant manifold $\mathscr{M}_{\varepsilon,\mathrm{r}}$ which is attracting for (22). The numerical integration is then stopped at the required value of the slow variable y. Note that, since $\mathscr{M}_{0,\mathrm{r}}$ is attracting in reverse time, the precise choice of the initial condition for the reverse time integration is not crucial as long as it is taken close to the critical manifold.

The previous definitions are especially relevant for purely transient dynamics when the increasing blowing pressure does not saturate in the bistability domain. In such a case, the system has no fixed points (at least it has none for $y < y_\mathrm{u}$) and we want to know when the bistability zone is crossed whether or not the original (i.e., non averaged) system oscillates significantly. In the case of musical instrument, this corresponds to the fact that a sound is produced (or not) during the transient. The case of a blowing pressure that saturates in the bistability domain is discussed in Section VI A.

Following the methodology described above, S is computed as the solution of (22) with the initial condition (23) (here this is $(x_0, y_0) = (x_3^\star(y_\mathrm{u}) = 0.95, y_\mathrm{u} = 1.34)$). The simulation is stopped when an arbitrary large value of $x(\tau)$ is reached. The resulting times series are shown in Fig. 3(a) (red solid and dashed lines for $x(\tau)$ and $y(\tau)$, respectively).

Fig. 3(b) shows the time integration of the direct time System (4) with an initial condition (IC) first in B_1 (in blue) and then in B_2 (in green). Both of these initial conditions are chosen close to S. In the case of IC $\in B_1$, we observe that $x(\tau)$ first rapidly approaches zero and remains equal to zero over time. In the case of IC $\in B_2$, similarly to the example in Fig. 2, after a first similar start transient, $x(\tau)$ remains close to zero for a moment and then moves away from it, taking a non-zero value for a period of time before falling back to zero. The first (resp. second) situation seems to correspond well to the case where the trajectory tends to follow $\mathscr{M}_{\varepsilon,\mathrm{a}_1}$ (resp. $\mathscr{M}_{\varepsilon,\mathrm{a}_2}$) when the bistability domain D is crossed. This appears more clearly in Fig. 3(c) in which the orbits previously computed are represented in the phase plane and superimposed to the critical manifold. The stream plot of the vector field Eq. (4) is also shown. The latter shows, for $y < y_\mathrm{u}$, that the orbits starting with an initial condition in the B_1 (resp. B_2), i.e., below (resp. above) S, end up following $\mathscr{M}_{\varepsilon,\mathrm{a}_1}$ (resp. $\mathscr{M}_{\varepsilon,\mathrm{a}_2}$).

To better understand what happens in the vicinity of the y-axis, a logarithmic scale is used in Fig. 3(d) for the ordinates. This example shows that very small amplitudes are encountered. In a real-world problems, residual noise would prevent reaching such low amplitudes. In the future, stochastic studies (similar to what was done in Ref. 10) would be relevant to complete this work.

Trajectories with initial conditions in B_1 (resp. B_2), but very close to S, follow it in a part of U_D before reaching quickly $\mathscr{M}_{\varepsilon,\mathrm{a}_1}$ (resp. $\mathscr{M}_{\varepsilon,\mathrm{a}_2}$). These special solutions can be seen as canards "without head"[54] (resp. "with head") and are represented in Fig. 3(c) by an orange (resp. magenta) streamline. In our application, clearly for long canards "without head" (see e.g. the orange streamline in Fig. 3(c)) a sound is produced during transient, in contradiction with the previous conclusions (i.e., a trajectory initialized in B_1 means no sound). Moreover, for long canards "with head" (see e.g. the magenta streamline in Fig. 3(c)) a sound is produced but it is short since the attracting branch $\mathscr{M}_{\varepsilon,\mathrm{a}_2}$ is reached close to the end of the bistability domain. We can therefore temper the previous conclusion (i.e., a trajectory initialized in B_1 means silence and in B_2 means sound during transient) by saying that it is valid for solutions of (4) that are not *canard* solutions. The latter represent a median behavior between silence and sound during transient. From this point of view, the transition from a perceptible sound to a real silence during transient does not therefore take place through the single trajectory S (the *maximum canard*) but through a family of *canards*. This situation has therefore common features with rate-induced tipping caused by crossing a rate-tipping quasithreshold, as reported by O'Sullivan *et al.*[45]. Even if canards are marginal solutions, to find out whether this subtlety could have an impact in the description of a real-life attack transient in single reed instrument, it would be interesting to quantify, for a given value of ε, the set of initial conditions corresponding to *canards* (or, for a given initial condition, the range of ε corresponding to these special solutions). This is left for future work.

Examples similar to those of Figs. 3(c) and 3(d) are shown in Fig. 4 for two other values of the parameter ε: $\varepsilon = 0.00366 < 0.0183$ (see Fig. 4(a)) and $\varepsilon = 0.0732 > 0.0183$ (see Fig. 4(b)). This shows that the smaller ε, the shorter (in terms of y) the above-mentioned transients, and the more visible the distinction between slow and fast epochs. In Fig. 4(b) in particular (top, blue line) the orbit is still relatively far from the $\mathscr{M}_{\varepsilon,\mathrm{a}_2}$ (the y-axis) when the upper bound of the bistability domain is reached. This highlights the limits of the approach for large values of ε. Nevertheless, the approach allows to interpret these borderline situations.

VI. DISCUSSION

A. Case of a blowing pressure saturating in the bistability domain

In this section the case where the blowing pressure tends towards a finite limit y_targ in the bistability domain is explored. More precisely, an exponential growth of the blowing pressure is considered using $g(y) = y_\mathrm{targ} - y$ (with $y_\mathrm{targ} \in D$) which yields

$$y(\tau) = y_\mathrm{targ} + (y_0 - y_\mathrm{targ})e^{-\tau}, \tag{24}$$

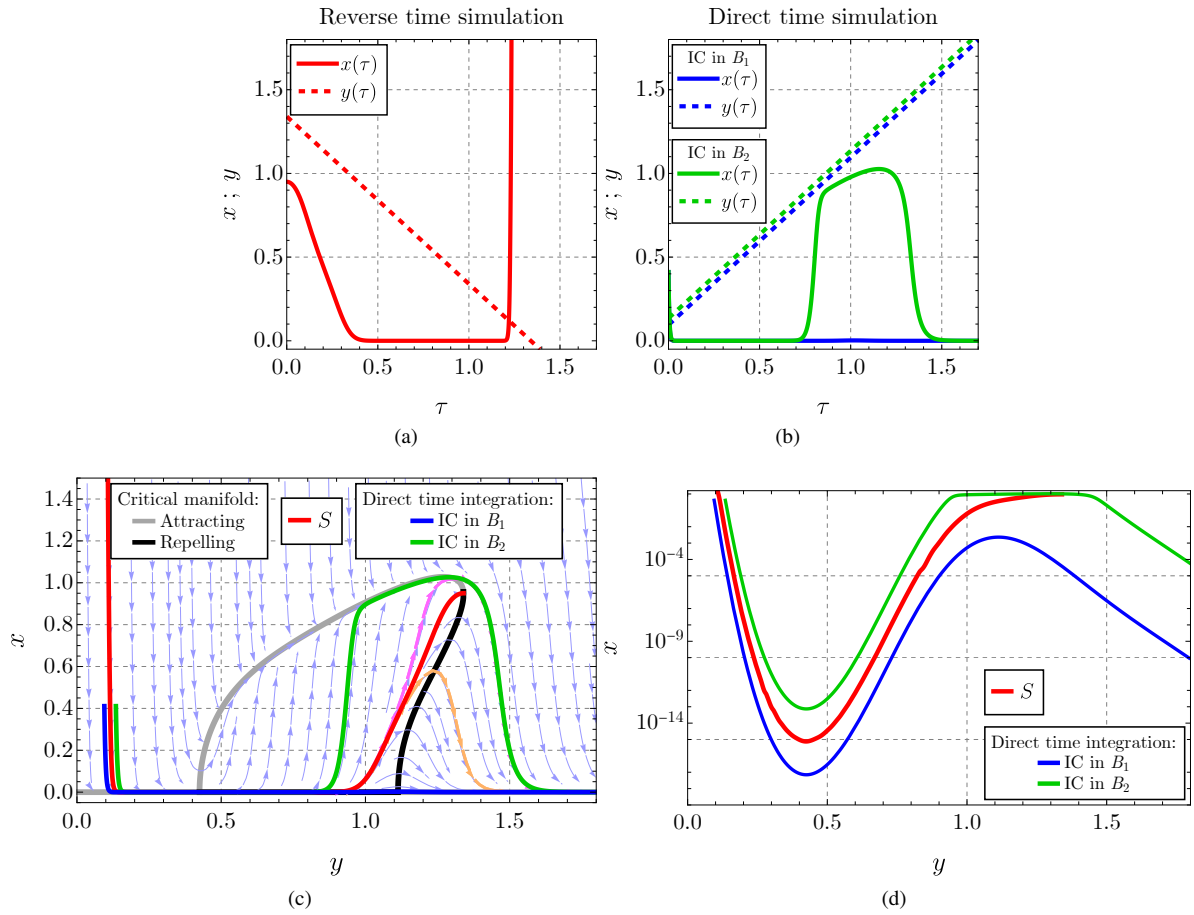

FIG. 3. (a) Times series of $x(\tau)$ (solid line) and $y(\tau)$ (dashed line) obtained by numerical integration of the reverse time System (22) with $g(y) = 1$ and an initial condition (IC) given by (23) (red). (b) Time series of the direct time System (4) with a IC first in B_1 (in blue) and in B_2 (in green) with B_1 and B_2 defined by Eqs. (19) and (20), respectively. (c) The corresponding orbits (same colors are used) in the phase plane and superimposed to the critical manifold. The orbit corresponding to the reverse time integration corresponds to the special solution S defined by Eq. (18). The stream plot of the vector field Eq. (4) with streamlines colored in light blue is also shown. Special streamlines corresponding to *canard* solutions "without head" and "with head" (i.e., following S, the *maximal canard*, in a part of U_D before leaving it on one side or the other) are represented in magenta and orange, respectively. (d) The same as in (c) but with a logarithmic scale for the ordinates. The parameters are given in Table I with in addition $\varepsilon = 0.0183$.

with again $y_0 = y(0)$. Written in the slow timescale τ, the system takes the following form

$$\varepsilon x' = f(x,y) \tag{25a}$$
$$y' = y_{\text{targ}} - y. \tag{25b}$$

This differs from the case studied so far, in which the pressure does not saturate. Here fixed points are solutions of $f(x,y) = 0$ and $y_{\text{targ}} - y = 0$, that leads to $f(x, y_{\text{targ}}) = 0$ and $x = x_i^\star(y_{\text{targ}})$ $(i = 1,2,3)$. Therefore, the points $P_i^\star = (x_i^\star(y_{\text{targ}}), y_{\text{targ}})$ $(i = 1,2,3)$ are the fixed points of Eq. (25). The Jacobian matrices $\mathbf{J}(P_i^\star)$ of (25) evaluated at each fixed point $P_i^\star$ are

$$\mathbf{J}(P_i^\star) = \begin{pmatrix} \dfrac{a_i^\star(y_{\text{targ}})}{\varepsilon} & \dfrac{\partial_y f(x_i^\star(y_{\text{targ}}), y_{\text{targ}})}{\varepsilon} \\ 0 & -1 \end{pmatrix} \tag{26}$$

whose eigenvalues are $\mu_1 = \frac{a_i^\star(y_{\text{targ}})}{\varepsilon}$ and $\mu_2 = -1$. Because $a_1^\star(y_{\text{targ}}) < 0$, $a_2^\star(y_{\text{targ}}) < 0$ and $a_3^\star(y_{\text{targ}}) > 0$ (see Eq. (12)), $P_1^\star$ and $P_2^\star$ are *nodes* (i.e., $\mu_1\mu_2 > 0$) and $P_3^\star$ is a *saddle* (i.e., $\mu_1\mu_2 < 0$). These classical definitions of nodes and saddle are taken from Ref. 50.

The problem therefore becomes a classic problem of finding the basins of attraction of stable fixed points of a two-dimensional system. In this case, the subsets B_1 and B_2 are indeed the basins of attraction of the stable equilibria $P_1^\star$ and $P_2^\star$ and S is the separatrix between these basins. This is the stable manifold of the unstable fixed point $P_3^\star$[16]. The latter is again computed using a time reversal simulation. The following equation

$$\varepsilon x' = -f(x,y) \tag{27a}$$
$$y' = -y_{\text{targ}} + y. \tag{27b}$$

is numerically integrated from initial condition chosen as a small perturbation of $P_3^\star$.

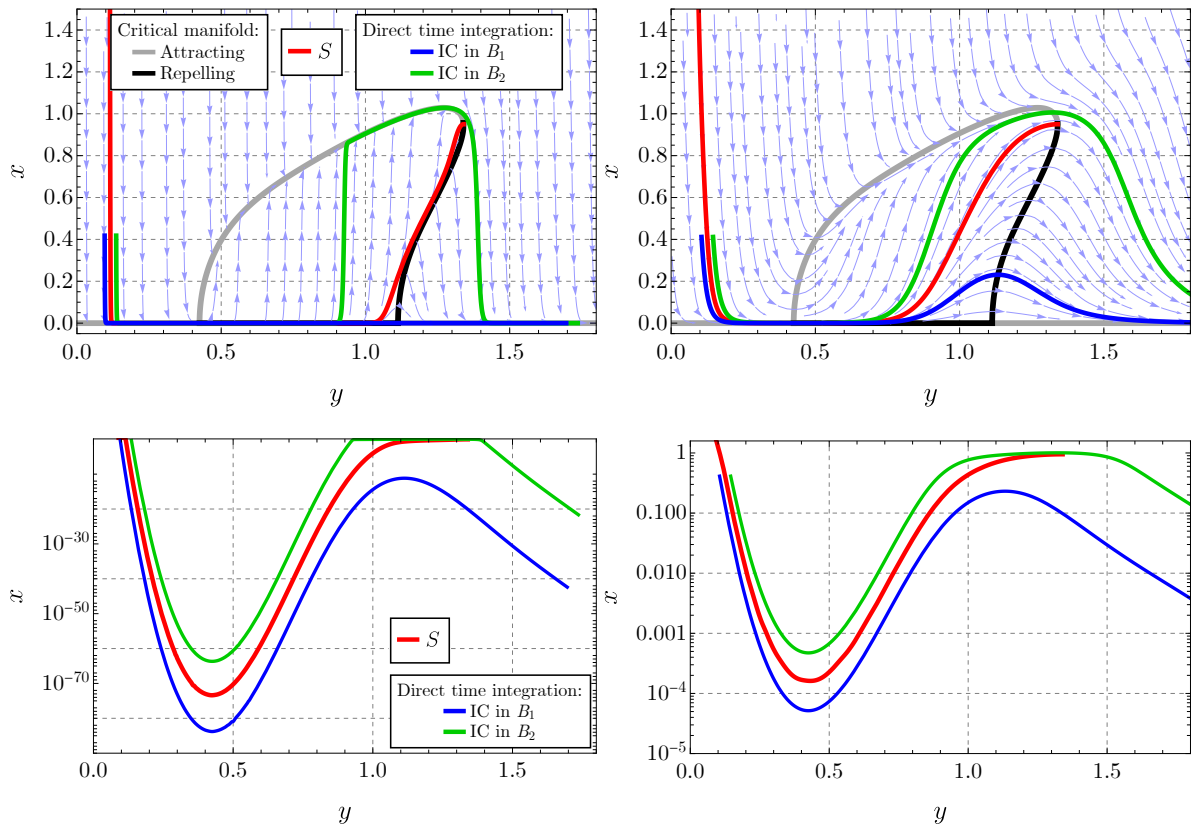

(a) $\hat{\varepsilon} = 10^{-4}$, $\varepsilon = 0.00366$. (b) $\hat{\varepsilon} = 2 \cdot 10^{-3}$, $\varepsilon = 0.0732$.

FIG. 4. The same figures as Figs 3(c) and 3(d) but with (a) $\hat{\varepsilon} = 10^{-4}$ and therefore $\varepsilon = 0.00366$ and (b) $\hat{\varepsilon} = 2 \cdot 10^{-3}$ and therefore $\varepsilon = 0.0732$.

An example is shown in Fig. 5. Figures 5(a) and 5(b) show similar representations as in Figs 3(c) and 3(d), respectively. In Fig. 5(a) the orange vertical line indicates the target value y_{targ} of the mouth pressure. Intersections between this vertical line and the critical manifold correspond to fixed points of (25). Importantly, the critical manifold is independent of the function $g(y)$ and therefore identical to the one previously obtained for a linear growth of y. Still in Fig. 5(a), a zoom near the unstable fixed point $P_3^\star$ is performed to highlight its stable manifold S.

Two orbits obtained by numerical integration of the direct time system Eq. (25) with (i) a IC first in B_1 (in blue) and (ii) in B_2 (in green) also appear in Fig. 5. The corresponding time series are plotted in Figs. 5(c) and 5(d), respectively. In the case of IC $\in B_1$, the orbit stays close to the y-axis for a moment and then moves away from it, follows the branch $\mathscr{M}_{\varepsilon,\mathrm{a}_1}$ of the critical manifold before stopping at $P_1^\star$. For IC $\in B_2$, it is the point $P_2^\star$ which ends up being reached. Here two different transients are observed before the fixed points are reached.

B. Case of more realistic models

This work aims to study the transient behavior of a simple model of reed instrument which reduces to a $(1,1)$-fast-slow system. However, more realistic models of reed instruments cannot be reduced to $(1,1)$-fast-slow systems. Working in the plane makes it easier to illustrate and understand the non trivial dynamic behavior we are interested in. However, the results obtained could be generalized to (m,n)-fast-slow systems. However, there are two things to bear in mind when the fast subsystem is more than one-dimensional. Firstly, the critical manifold is also more than one-dimensional and it can be attracting (if all eigenvalues of the Jacobian matrix of the fast subsystem evaluated on the critical manifold have negative real parts), repelling (if all the eigenvalues have positive reals parts) and *saddle-type* (if there are eigenvalues with negative real parts and others with positive real parts). Previous definitions are taken from Ref. 34 (Chap. 3). Saddle-type invariant manifolds cannot be obtained by reversing the time, as presented above for a purely repelling manifold. Indeed, a saddle-type manifold in direct time remains saddle-type in reverse time. In this case, advanced numerical methods must be used to compute the equivalent of the solution S, as proposed for example by Guckenheimer and Kuehn[30] and Farjami *et al.*[23]. The second thing to consider is that the fast subsystem can have other types of solutions than equilibria; such as periodic or quasiperiodic solutions. The complete bifurcation diagram of the fast subsystem (including periodic solutions and if possible quasiperiodic solutions) is not anymore the critical manifold of the studied (m,n)-fast-slow system which in-

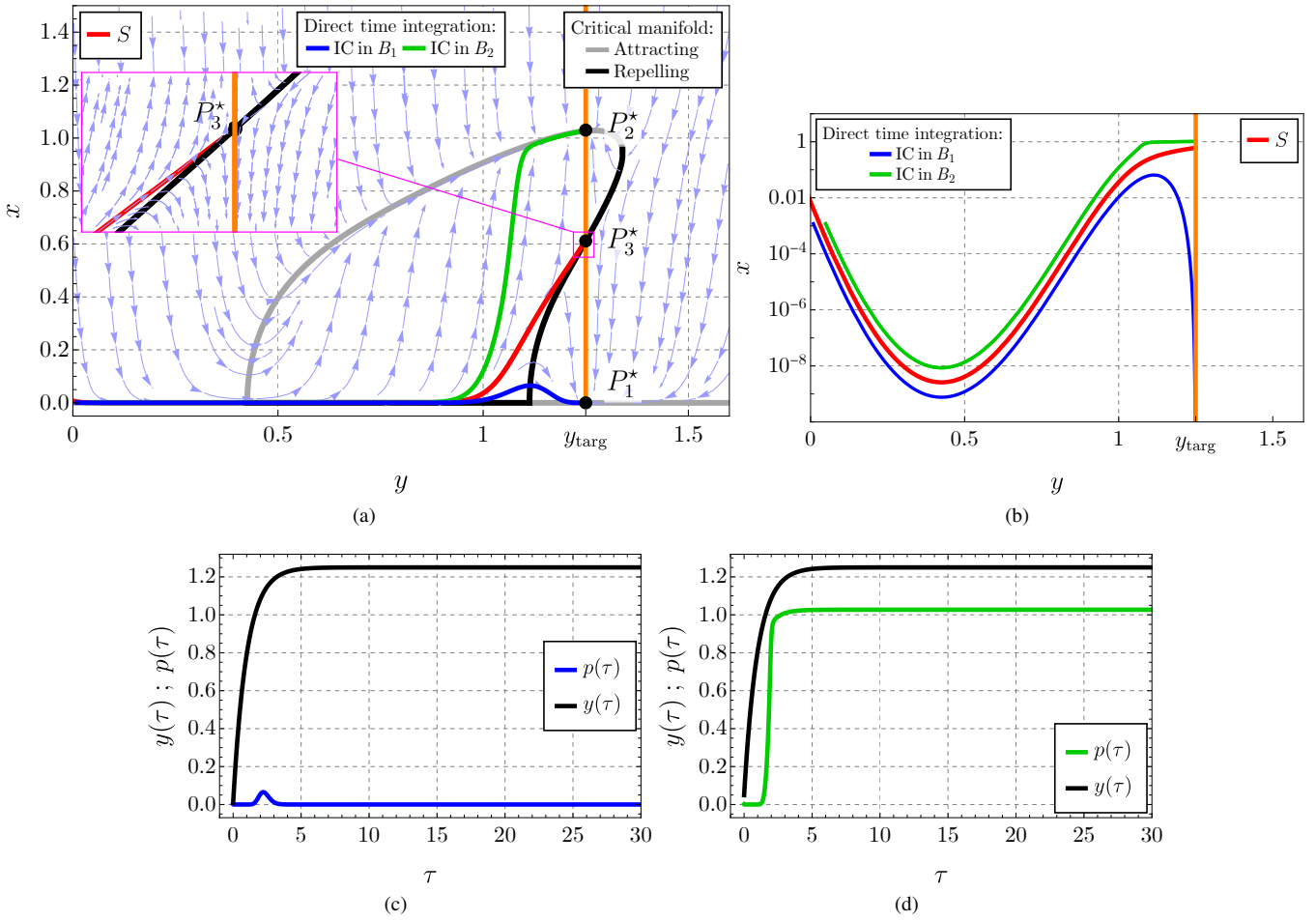

FIG. 5. (a) Orbit obtained by the numerical integration of the reverse time System (22) with $g(y) = y_{\text{targ}} - y$ and an initial condition (IC) chosen as a small perturbation of the non trivial fixed point $P_3^\star$ (in red). This special solution S which is here the stable manifold of the unstable fixed point $P_3^\star$. Two orbits obtained by the numerical integration of direct time system Eq. (25): with a IC first in B_1 (in blue) and in B_2 (in green). The corresponding time series are plotted in Figs. 5(c) and 5(d), respectively. The stream plot of the vector field Eq. (4) with streamlines colored in light blue is also shown is also shown. (b) The same as in (a) but with a logarithmic scale for the ordinates. The parameters are given in Table I with in addition $\varepsilon = 0.0732$, $y_{\text{targ}} = 1.25$.

cludes only the equilibrium solutions. In a (m,n)-fast-slow system, invariant manifolds associated to quasiperiodic solutions of the fast subsystem are more complicated to deal with, both analytically and computationally. However, periodic solutions can be treated in the same way as equilibrium solutions. First, because theoretically Berglund[12] proposes an analogue of Fenichel's theorem on the existence of an invariant manifold tracking families of periodic orbits and also because periodic solutions are easy to compute numerically. As in the case of equilibrium solutions, for the time reversal method to be used, the invariant manifold considered to compute S must be repelling. For periodic solutions, that means that $m-1$[42] of the *Floquet multipliers* associated with the periodic solution under consideration have modulus strictly larger than one (see e.g. Ref. 50, Chap. 7, for details about local stability of periodic solutions).

We provide here an illustration for the original System (A7) (replacing γ by $y(t')$ and switching from t' to t, see Appendix A), a $(2,1)$-fast-slow system (globally 3-dimensional) since the 1-dimensional complex Eq. (A13) is a two-dimensional real equation.

As mentioned above, the trivial fixed point of the fast subsystem (10) associated to the averaged dynamics (3) is the equilibrium solution of the original non-averaged dynamics (A7) and non trivial fixed points correspond to periodic solutions of (A7). In the bistability domain the fast subsystem associated to the original dynamics has thus a stable equilibrium solution, a stable and an unstable periodic solutions. The manifolds corresponding to these periodic solutions are represented in Fig. 6 by gray and black surfaces in the $(y,p,\dot{p})$-space, respectively. In practice these manifolds, which also represent the bifurcation diagram of the original dynamical system, are deduced from the critical manifold of Eq. (3). Indeed, in the $(p,\dot{p})$-plane periodic solutions of the non-averaged dynamics (A7) is a circle whose radius is equal to the value of the corresponding fixed point of Eq. (3). The manifolds of the periodic solutions of the latter are then obtained by rotation of the critical manifold of Eq. (3) around

the y-axis.

The equivalent of the solution S (see Eq. (18)) for the original system (A7) (also denoted here as S for the sake of conciseness) is here the extension of a two-dimensional repelling slow invariant manifold associated to the unstable periodic solution of the fast subsystem. In a two-dimensional system an unstable periodic solution is associated to two Floquet multipliers, one is unity[42] and the other has modulus larger than one. Therefore, the associated invariant manifold is repelling and the reverse time procedure can be used.

In Fig. 6 the solution S is shown in red in the $(y, p, \dot{p})$-space. Although S is now two-dimensional, here we computed only one solution of the time-reversed system for initial conditions on the periodic solution at $y = y_u$. Here, oscillations are sufficiently fast for S to be represented correctly by a single periodic orbit. Here also S splits the three-dimensional phase space into two subsets, here again denoted as B_1 and B_2 for the sake of conciseness.

Results of time-domain simulation of the $(2,1)$-fast-slow original system (in direct time) with two different sets of initial conditions, one in B_1 (in blue) and the second one in B_2 (in green) are also shown in Fig. 6. The parameters and IC are the same as in Fig. 3 (same parameters and initial conditions) and similar observations can be made: when IC $\in B_1$, the orbit first winds around the y-axis and remains in the vicinity of it. Conversely, when IC $\in B_2$, after a first similar start transient, the orbits stays on vicinity of the y-axis for a while and then moves away to reach the manifold associated to the stable periodic solution. The simulation is carried out over a shorter period of time than in Fig. 3. This is why we do not observe the orbit falling back to zero.

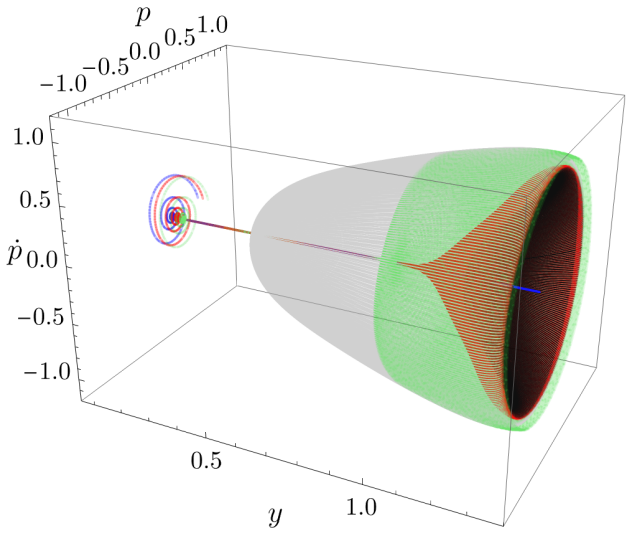

FIG. 6. The manifolds of (A7) associated to the stable and unstable periodic solutions of the fast subsystem of the original non-averaged dynamics (A7) are depicted by gray and black surfaces, respectively. Orbit obtained by the numerical integration of the reverse time system associated to Eq. (A7) (replacing γ by $y(t')$ and switching from t' to t, see Appendix A) and an IC on the circle representing the periodic solution in the $(p, \dot{p})$-plane at $y = y_u$ (in red). This represents the solution S of the 3-dimensional original dynamics. Two orbits obtained by the numerical integration of direct time system: with a IC first in B_1 (in blue) and in B_2 (in green). Same parameters as in Fig. 3.

VII. CONCLUSION

In this paper the behavior of a class of one-dimensional non-autonomous dynamical systems has been investigated. These systems are obtained by slowly varying over time the bifurcation parameter of the corresponding autonomous systems with constant bifurcation parameter (referred to as the fast subsystem throughout this article). More precisely, we focused on the case where the time-varying parameter crosses a bistability domain of the corresponding autonomous system. This is motivated by the application context of self-sustained musical instruments, with a focus here on a simple model of reed instrument (such as the clarinet). Indeed, initial acoustical transients (at the beginning of a note) are known to be of crucial importance in a musical context and they depend directly on attack transients on the playing parameter as controlled by the musician.

In the bistability domain, the non-autonomous system has attracting invariant manifolds (resp. a repelling invariant manifold) associated with the two stable branches (resp. unstable branch) of the bifurcation diagram of the corresponding autonomous system. We have shown that knowledge of a single solution of the system under study (in which the time-varying parameter is considered as another state variable) can be used to describe its global behavior. This solution, whose section in the bistability domain is the repelling invariant manifold, splits the phase space into two subsets which have the following feature: a solution with an initial condition in one of these subsets ends up following one of the attracting manifolds and a solution with an initial condition in the other subset ends up following the other attracting manifold. In practice, the threshold solution has been computed using a numerical reverse time integration with relevant initial conditions.

From an application point of view, this allows to predict the nature of the acoustical transient associated to a given attack transient on the control parameter, for example in the case considered in this article to discriminate between transients where no sound is produced and transients where a sound is produced. As such, these results might pave the way towards a better understanding and modeling of the transient dynamics of musical instruments which may be of interest for virtual prototyping and instrument making.

As a first perspective, still on low dimensional systems, it would be interesting to develop analytical methods that would make it possible to relate the characteristics of the time-varying parameter to the nature of the observed regime. Moreover, in the context of real-life applications, the method should be extended to more complex dynamical systems. In this case, if the solutions (stable and unstable) of the multistable autonomous system are more complex than equilibria, the challenge will be to detect the unstable solutions to then

deduce the possible threshold solution of the non-autonomous system. This implies to use more advanced numerical approaches such as continuation methods. Secondly, multistable systems and systems with time-varying parameter undergoing so-called bifurcation delay are known to be very sensitive to noise. Therefore, the influence of noise should be studied in the future.

From a more general point of view, we believe that the results and method presented in the article might be of interest beyond the specific application considered here, for example in physics, neurosciences or climate sciences. In particular, our results strongly relate to the phenomena of critical transitions, rate-induced and bifurcation-induced tipping which have attracted considerable attention in the last years, but with the focus here on the transient dynamics.

DATA AVAILABILITY STATEMENT

The data that support the findings of this study are available from the corresponding author upon reasonable request.

Appendix A: Derivation of the model

1. Classical single reed instrument model

Sound production by single reed instruments is classically modeled through the nonlinear coupling between two linear components[5,15,27]: the reed and the air-column inside the instrument. While blowing air through the reed channel into the instrument, the instrumentalist provides a quasi-static source of energy. The instrument and the player constitute an autonomous dynamical system. When the trivial equilibrium solution of this system becomes unstable, a sound is produced[26,51,58].

Since the lowest resonance frequency of the reed is one order of magnitude higher than the sound frequency for many notes, the reed is often modeled as a lossless stiffness spring[4,44]. Therefore its position relative to rest is proportional to the pressure drop across the reed, i.e., the pressure difference between the mouth and the mouthpiece of the instrument. The linear pressure response of the air column P to the volume flow U through the reed channel is given in the frequency domain through the input impedance of the air column Z

$$P(\omega) = Z(\omega)U(\omega), \tag{A1}$$

where ω is the angular frequency. We point out that the model presented in the appendix already considers a dimensionless pressure and flow (see Chap. 9 of Ref. 15 for more details on the model).

The contribution at the input of the instrument of the (infinite) series of modes of the air column is taken into account in $Z(\omega)$. For computational reasons, the series is truncated to N modes, where N is an integer:

$$Z(\omega) = \sum_{n=1}^{N} Z_n \frac{j\varepsilon_n\omega_n\omega}{\omega_n^2 + j\varepsilon_n\omega_n\omega - \omega^2}, \tag{A2}$$

with Z_n, ω_n and ε_n the modal parameters, respectively the modal factor, the resonance angular frequency and the inverse of the quality factor of the n^{th} peak of the impedance (corresponding to the n^{th} mode of the air column). Eq. (A2) can be written in the time domain

$$d_{t''t''}p_n + \varepsilon_n\omega_n d_{t''}p_n + \omega_n^2 p_n = Z_n\varepsilon_n\omega_n d_{t''}u, \quad \forall n \in [1,N], \tag{A3}$$

in which t'' is used to denote the original timescale, u is the inverse Fourier transform of U and p_n is such that $p = \sum_{i=1}^{N} p_n$, where p is the inverse Fourier transform of P[51] and corresponds to the time evolution of the mouthpiece pressure.

Through Bernoulli's principle, the volume flow through the reed channel u is related nonlinearly to the reed channel opening and the pressure difference between the mouth and the mouthpiece[19,31]

$$u = \hat{F}(p,\gamma) = \zeta(1+p-\gamma)\sqrt{|\gamma-p|}\,\mathrm{sgn}(\gamma-p)H(1+p-\gamma) \tag{A4}$$

where H is the Heaviside function, γ is the dimensionless pressure in the mouth of the musician and ζ a dimensionless parameter accounting for many embouchure parameters. The parameters γ and ζ are the *control (or bifurcation) parameters* of the model. The relation (A4) is called the nonlinear characteristic (NLC) of the instrument exciter. In this work a polynomial fitting of the function $\hat{F}(p,\gamma)$ (see Eq. (A4)), denoted $F(p,\gamma)$, is obtained using the function `InterpolatingPolynomial` of the Mathematica software[59] (see Fig. 7).

Using the function $F(p,\gamma)$, Eq. (A3) can be written using

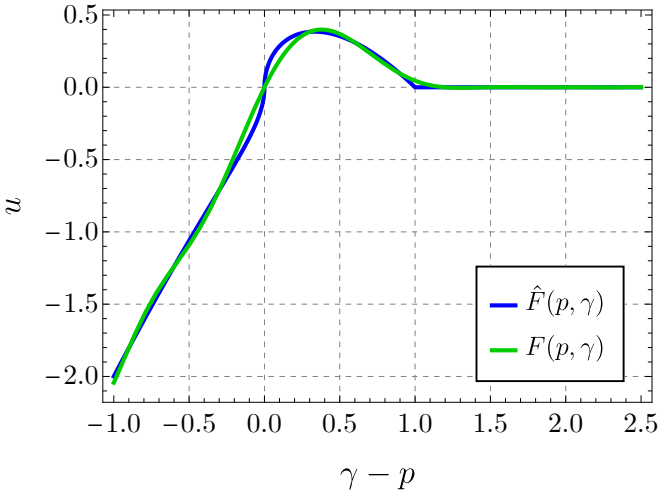

FIG. 7. Comparison between the function $\hat{F}(p,\gamma)$ given by Eq. (A4) (blue line) and its polynomial fitting $F(p,\gamma)$ (green line) as functions of the pressure difference $\gamma - p$.

only the pressure p as follows

$$d_{t''t''}p_n + \varepsilon_n \omega_n d_{t''}p_n + \omega_n^2 p_n - Z_n \varepsilon_n \omega_n d_{t''}p_n \partial_p F(p,\gamma) = 0, \quad \forall n \in [1,N]. \tag{A5}$$

A minimal model of a reed instrument including a single mode of the air-column is obtained by stating $N = 1$. In this case (A5) becomes

$$d_{t''t''}p + \varepsilon_1 \omega_1 d_{t''}p + \omega_1^2 p - Z_1 \varepsilon_1 \omega_1 d_{t''}p \partial_p F(p,\gamma) = 0 \tag{A6}$$

In this case ($N = 1$), since $p_1 = p$, p_1 is replaced by p in Eq. (A6). This is clearly a minimal yet useful model of sound production in reed instruments. Indeed, it takes into account the two main control parameters, γ et ζ, adjusted by the musician and describes the physical mechanism through which sound emerges from the trivial equilibrium (i.e. silence) when a resonance of the air column is excited by an incoming flow. We finally introduce the dimensionless time $t' = \omega_1 t''$, so Eq. (A6) takes the form of the following self-excited oscillator

$$d_{t't'}p + \varepsilon_1 h(p, d_{t'}p, \gamma) + p = 0. \tag{A7}$$

where

$$h(p, d_{t'}p, \gamma) = d_{t'}p\,(1 - Z_1 \partial_p F(p,\gamma)). \tag{A8}$$

2. Averaged dynamics with a slowly time-varying control parameter

Eq. (A7), in the phase space $(p, d_{t'}p)$, is transformed to a slowly varying system using the following complex representation introducing a new variable ξ as

$$\xi e^{jt'} = d_{t'}p + jp \tag{A9}$$

with $j^2 = -1$. Combining Eq. (A9) and its complex conjugate yields the expressions of p and $d_{t'}p$ as functions of ξ

$$p = \frac{\xi e^{jt'} - \xi^* e^{-jt'}}{2j}, \tag{A10}$$

$$d_{t'}p = \frac{\xi e^{jt'} + \xi^* e^{-jt'}}{2}, \tag{A11}$$

where ξ^* is the complex conjugate of ξ. Deriving Eq. (A9) with respect to t' and using Eq. (A11) give $d_{t't'}p$ as

$$d_{t't'}p = d_{t'}\xi e^{jt'} + j\xi e^{jt'} - \frac{j}{2}\left(\xi e^{jt'} + \xi^* e^{-jt'}\right). \tag{A12}$$

Substituting Eqs. (A10), (A11) and (A12) into Eq. (A7) yields the following complex non-autonomous system

$$d_{t'}\xi = -\varepsilon_1 h\left(\frac{\xi e^{jt'} - \xi^* e^{-jt'}}{2j}, \frac{\xi e^{jt'} + \xi^* e^{-jt'}}{2}, \gamma\right) e^{-jt'}. \tag{A13}$$

Then, stating $\xi = xe^{j\varphi}$ and $\phi = t' + \varphi$ and separating real and imaginary parts of each side of Eq. (A13) gives

$$d_{t'}x = -\varepsilon_1 h(x\sin\phi, x\cos\phi, \gamma)\cos\phi, \tag{A14a}$$

$$d_{t'}\phi = 1 + \varepsilon_1 h(x\sin\phi, x\cos\phi, \gamma)\frac{\sin\phi}{x}. \tag{A14b}$$

Since $0 < \varepsilon_1 \ll 1$, Eq. (A14) is simplified by means of an averaging method (see Chap. 7 of Ref. 49) to

$$d_{t'}x = \varepsilon_1 f(x,\gamma), \tag{A15a}$$

$$d_{t'}\phi = 1 \tag{A15b}$$

where x and ϕ are uncoupled and

$$f(x,\gamma) = -\frac{1}{2\pi}\int_0^{2\pi} h(x\sin\alpha, x\cos\alpha, \gamma)\cos\alpha d\alpha. \tag{A16}$$

Details on the averaging procedure are provided in Section B.

The integral in Eq. (A16) is generally hard to solve analytically, except if the function h is assumed to have a polynomial form. This is the case here using the polynomial fitting $F(p,\gamma)$ of the NLC.

The dynamics of the mouth pressure (now denoted y) is finally added as $d_{t'}y = \hat{\varepsilon} g(y)$. Then, assuming $\hat{\varepsilon}/\varepsilon_1 \ll 1$, switching the time from t' to $t = \varepsilon_1 t'$ and using the notation $\dot{\{\}} = d_t\{\}$, the following system is obtained

$$\dot{x} = f(x,y) \tag{A17a}$$

$$\dot{y} = \varepsilon g(y) \tag{A17b}$$

where ε is defined as

$$\varepsilon = \frac{\hat{\varepsilon}}{\varepsilon_1} \tag{A18}$$

which is the relevant small parameter to use for this model.

Appendix B: Details on the averaging procedure

Omitting here, for the sake of clarity, the dependence in γ, and introducing

$$X(x,\phi) = -h(x\sin\phi, x\cos\phi, \gamma)\cos\phi, \tag{B1a}$$

$$\Omega(x,\phi) = h(x\sin\phi, x\cos\phi, \gamma)\frac{\sin\phi}{x}, \tag{B1b}$$

Eq. (A14) becomes

$$d_{t'}x = \varepsilon_1 X(x,\phi), \tag{B2a}$$

$$d_{t'}\phi = 1 + \varepsilon_1 \Omega(x,\phi). \tag{B2b}$$

The latter is a $(1,1)$-fast-slow systems with t' the fast timescale, x the slow variable and ϕ the fast variable. The principle of the average procedure (see Chap. 7 of Ref. 49), consists in assuming the following form for the variable x

$$x = v + \varepsilon_1 u(v,\phi) \tag{B3}$$

with $u(v,\phi)$ a function $2\pi-$periodic in ϕ.

Using Eq. (B3) and

$$d_{t'}u = (1+\varepsilon_1\Omega(v+\varepsilon_1 u,\phi))\,\partial_\phi u + d_{t'}v\partial_v u, \tag{B4}$$

Eq. (B2a) becomes

$$d_{t'}v(1+\varepsilon_1\partial_v u)+\varepsilon_1\,(1+\varepsilon_1\Omega(v+\varepsilon_1 u,\phi))\,\partial_\phi u = \varepsilon_1 X(v+\varepsilon_1 u,\phi). \tag{B5}$$

Each ε_1-dependent function in (B5) is expanded in a first-order Taylor series around $\varepsilon_1 = 0$, that yields

$$d_{t'}v+\varepsilon_1\left(1+\varepsilon_1\Omega(v,\phi)+\mathscr{O}(\varepsilon_1^2)\right)(1-\varepsilon_1\partial_v u+\mathscr{O}(\varepsilon_1^2))\partial_\phi u = \left(\varepsilon_1 X(v,\phi)+\mathscr{O}(\varepsilon_1^2)\right)(1-\varepsilon_1\partial_v u+\mathscr{O}(\varepsilon_1^2)) \tag{B6}$$

which simplifies into

$$d_{t'}v = \varepsilon_1\left(X(v,\phi)-\partial_\phi u\right)+\mathscr{O}(\varepsilon_1^2) \tag{B7}$$

Then one assumes a function $u(v,\phi)$ which satisfies the following equation

$$\partial_\phi u = X(v,\phi)-f(v). \tag{B8}$$

Integrating (B8) with respect to ϕ from 0 to 2π and because $u(v,\phi)$ is 2π-periodic in ϕ we obtain

$$f(v) = \frac{1}{2\pi}\int_0^{2\pi} X(v,\alpha)d\alpha, \tag{B9}$$

and then $f(v)$ is the average of $X(v,\phi)$ as defined in Eq. (A16).

Substituting (B8) into (B7) and adding Eq. (B2b) we obtain a simplified dynamical system with the following form

$$d_{t'}v = \varepsilon_1 f(v)+\mathscr{O}(\varepsilon_1^2) \tag{B10a}$$
$$d_{t'}\phi = 1+\mathscr{O}(\varepsilon_1). \tag{B10b}$$

Finally, consistently with $0<\varepsilon_1\ll 1$, we have $\varepsilon_1 f(v)+\mathscr{O}(\varepsilon_1^2)\approx\varepsilon_1 f(v)$, $1+\mathscr{O}(\varepsilon_1)\approx 1$ and $v\approx x$ and therefore Eq. (A15) is proven.

[1] Alkhayuon, H. M.and Ashwin, P., "Rate-induced tipping from periodic attractors: Partial tipping and connecting orbits," Chaos: An Interdisciplinary Journal of Nonlinear Science **28**, 033608 (2018).

[2] Ashwin, P., Perryman, C., and Wieczorek, S., "Parameter shifts for nonautonomous systems in low dimension: bifurcation- and rate-induced tipping," Nonlinearity **30**, 2185–2210 (2017).

[3] Ashwin, P., Wieczorek, S., Vitolo, R., and Cox, P., "Tipping points in open systems: bifurcation, noise-induced and rate-dependent examples in the climate system," Philosophical Transactions of the Royal Society A: Mathematical, Physical and Engineering Sciences **370**, 1166–1184 (2012).

[4] Backus, J., "Small-vibration theory of the clarinet," J. Acoust. Soc. Am. **35**, 305–313 (1963).

[5] Benade, A. H., *Fundamentals of musical acoustics*, edited by O. U. Press (Oxford University Press, 1976).

[6] Benoît, E., "Dynamic bifurcations," in *Lect. Notes Math.*, Vol. 1493 (Springer, Actes de la condérence tenue à Luminy, Marseilles, France, du 5 au 10 mars 1990).

[7] Bergeot, B., Almeida, A., Vergez, C., and Gazengel, B., "Prediction of the dynamic oscillation threshold in a clarinet model with a linearly increasing blowing pressure," Nonlinear Dynamics **73**, 521–534 (2013).

[8] Bergeot, B., Almeida, A., Vergez, C., and Gazengel, B., "Prediction of the dynamic oscillation threshold in a clarinet model with a linearly increasing blowing pressure: influence of noise," Nonlinear Dynamics **74**, 591–605 (2013).

[9] Bergeot, B., Almeida, A., Vergez, C., Gazengel, B., and Ferrand, D., "Response of an artificially blown clarinet to different blowing pressure profiles," J. Acoust. Soc. Am. **135**, 479–490 (2014).

[10] Bergeot, B.and Vergez, C., "Analytical prediction of delayed hopf bifurcations in a simplified stochastic model of reed musical instruments," Nonlinear Dynamics **107**, 3291–3312 (2022).

[11] Berglund, N., "Dynamic Bifurcations: Hysteresis, Scaling Laws and Feedback Control," Progress of Theoretical Physics Supplement **139**, 325–336 (2000).

[12] Berglund, N.and Gentz, B., *Noise-induced phenomena in slow-fast dynamical systems, A sample-paths approach*, Probability and its Applications (New York) (Springer-Verlag London Ltd., 2006) (In this reference the *critical manifold* is called *slow manifold*).

[13] Berglund, N.and Gentz, B., "Stochastic dynamic bifurcations and excitability," Stochastic Methods in Neuroscience (2010), 10.1093/acprof:oso/9780199235070.003.0003.

[14] Berglund, N.and Landon, D., "Mixed-mode oscillations and interspike interval statistics in the stochastic FitzHugh–Nagumo model," Nonlinearity **25**, 2303–2335 (2012).

[15] Chaigne, A.and Kergomard, J., *Acoustics of Musical Instruments*, Modern Acoustics and Signal Processing (Springer-Verlag New York, 2016).

[16] Chiang, H.-D., Hirsch, M., and Wu, F., "Stability regions of nonlinear autonomous dynamical systems," IEEE Transactions on Automatic Control **33**, 16–27 (1988).

[17] Colinot, T., Guillemain, P., Vergez, C., Doc, J.-B., and Sanchez, P., "Multiple two-step oscillation regimes produced by the alto saxophone," The Journal of the Acoustical Society of America **147**, 2406–2413 (2020).

[18] Colinot, T., Vergez, C., Guillemain, P., and Doc, J.-B., "Multistability of saxophone oscillation regimes and its influence on sound production," Acta Acustica **5**, 33 (2021).

[19] Dalmont, J. P., Gilbert, J., and Ollivier, S., "Nonlinear characteristics of single-reed instruments: Quasistatic volume flow and reed opening measurements," J. Acoust. Soc. Am. **114**, 2253–2262 (2003).

[20] Doc, J.-B., Vergez, C., and Missoum, S., "A minimal model of a single-reed instrument producing quasi-periodic sounds," Acta Acustica united with Acustica **100**, 543–554 (2014).

[21] Ernoult, A.and Fabre, B., "Temporal characterization of experimental recorder attack transients," The Journal of the Acoustical Society of America **141**, 383–394 (2017).

[22] Ernoult, A., Fabre, B., Terrien, S., and Vergez, C., "Experimental study of attack transients in flute-like instruments," in *International Symposium on Musical Acoustics* (2014).

[23] Farjami, S., Kirk, V., and Osinga, H. M., "Computing the stable manifold of a saddle slow manifold," SIAM Journal on Applied Dynamical Systems **17**, 350–379 (2018), https://doi.org/10.1137/17M1132458.

[24] Fenichel, N., "Geometric singular perturbation theory for ordinary differential equations," Journal of Differential Equations **98**, 53–98 (1979).

[25] Feudel, U., Pisarchik, A. N., and Showalter, K., "Multistability and tipping: From mathematics and physics to climate and brain—Minireview and preface to the focus issue," Chaos: An Interdisciplinary Journal of Nonlinear Science **28**, 033501 (2018).

[26] Fletcher, N., "Nonlinear theory of musical wind instruments," Applied Acoustics **30**, 85 – 115 (1990).

[27] Fletcher, N. H.and Rossing, T. D., *The physics of musical instruments* (Springer-Verlag, New York, 1991).

[28] Gilbert, J., Maugeais, S., and Vergez, C., "Minimal blowing pressure allowing periodic oscillations in a simplified reed musical instrument model: Bouasse-Benade prescription assessed through numerical continuation," Acta Acustica **4**, 12 (2020).

[29] Gourc, E., Vergez, C., Mattei, P.-O., and Missoum, S., "Nonlinear dynamics of the wolf tone production," Journal of Sound and Vibration **516**, 116463 (2022).

[30] Guckenheimer, J.and Kuehn, C., "Computing slow manifolds of saddle type," SIAM Journal on Applied Dynamical Systems **8**, 854–879 (2009), https://doi.org/10.1137/080741999.

[31] Hirschberg, A., "Aero-acoustics of wind instruments," in *Mechanics of musical instruments by A. Hirschberg/ J. Kergomard/ G. Weinreich*, Vol. 335 of *CISM Courses and lectures* (Springer-Verlag, 1995) Chap. 7, pp. 291–361.

[32] Jones, C. K., "Geometric singular perturbation theory," in *Dynamical Systems*, Lecture Notes in Mathematics, Vol. 1609, edited by R. Johnson

(Springer Berlin Heidelberg, 1995) pp. 44–118.
[33] Kuehn, C., "Multiple time scale dynamics," (Springer International Publishing, 2015) Chap. 12, 1st ed.
[34] Kuehn, C., *Multiple Time Scale Dynamics*, 1st ed., edited by S. Antman, Applied Mathematical Sciences, Vol. 191 (Springer International Publishing, 2015).
[35] Mattéoli, R., Gilbert, J., Terrien, S., Dalmont, J.-P., Vergez, C., Maugeais, S., and Brasseur, E., "Diversity of ghost notes in tubas, euphoniums and saxhorns," Acta Acustica **6**, 32 (2022).
[36] Normally, a musical note corresponds to a periodic solution. However, the instrument model we are going to study is averaged, therefore for it a musical note is non-zero equilibrium corresponding to the amplitude of the periodic solution of the original model.
[37] *Normally* means that each point of $\mathscr{M}_0$ must be hyperbolic only in the the direction normal (i.e., non tangent) to itself (see e.g. Definition 2.3.4 and the text below of Ref. 34).
[38] To be understood in the sense of the Hausdorff distance (see e.g. Chap. 3 of Ref. 34)..
[39] $\mathscr{M}_\varepsilon$ is called invariant (locally in I) under the flow, if $(x_0, y_0) \in \mathscr{M}_\varepsilon$ implies that $(x(t), y(t)) \in \mathscr{M}_\varepsilon$ as long as $y(t) \in I$ holds.
[40] Remember that for a $(1,1)$-fast-slow system, the critical manifold represents the equilibrium solutions of the corresponding autonomous system, i.e, the fast subsystem (10).
[41] The behavior of a $(1,1)$-fast-slow system near a non hyperbolic point of the critical manifold can be analytically studied by means of the methodology developed by Berglund *et al.*[12] which consists in determining the *scaling law* of the system, i.e., the dependance of the system in the parameter ε in the neighborhood of the non hyperbolic point. This is not the purpose of the present paper because this analytical method cannot be extended for higher dimensional phase spaces.
[42] A periodic solution of an m-dimensional fast subsystem is associated to m Floquet multipliers but one is always unity (see Lemma 7.3 of Ref. 50).
[43] O'Keeffe, P. E.and Wieczorek, S., "Tipping phenomena and points of no return in ecosystems: beyond classical bifurcations," SIAM Journal on Applied Dynamical Systems **19**, 2371–2402 (2020).
[44] Ollivier, S., Dalmont, J. P., and Kergomard, J., "Idealized models of reed woodwinds. part 1 : Analogy with the bowed string," Acta. Acust. Acust. **90**, 1192–1203 (2004).
[45] O'Sullivan, E., Mulchrone, K., and Wieczorek, S., "Rate-induced tipping to metastable Zombie fires," Proceedings of the Royal Society A: Mathematical, Physical and Engineering Sciences **479**, 20220647 (2023).
[46] Pàmies-Vilà, M., Hofmann, A., and Chatziioannou, V., "Analysis of tonguing and blowing actions during clarinet performance," Frontiers in psychology **9**, 366042 (2018).
[47] Ritchie, P. D., Alkhayuon, H., Cox, P. M., and Wieczorek, S., "Rate-induced tipping in natural and human systems," Earth System Dynamics **14**, 669–683 (2023).
[48] Saldanha, E.and Corso, J. F., "Timbre cues and the identification of musical instruments," The Journal of the Acoustical Society of America **36**, 2021–2026 (1964).
[49] Sanders, J. A., Verhulst, F., and Murdock, J. A., *Averaging methods in nonlinear dynamical systems*, 2nd ed., Applied mathematical sciences No. v. 59 (Springer, New York, 2007).
[50] Seydel, R., *Practical Bifurcation and Stability Analysis*, 3rd ed., Interdisciplinary Applied Mathematics, Vol. 5 (Springer, 2010).
[51] Silva, F., Kergomard, J., Vergez, C., and Gilbert, J., "Interaction of reed and acoustic resonator in clarinet-like systems," J. Acoust. Soc. Am. **124**, 3284–3295 (2008).
[52] Terrien, S., Vergez, C., de La Cuadra, P., and Fabre, B., "Experimental analysis of non-periodic sound regimes in flute-like musical instruments," The Journal of the Acoustical Society of America **149**, 2100–2108 (2021).
[53] Tredicce, J. R., Lippi, G. L., Mandel, P., Charasse, B., Chevalier, A., and Picqué, B., "Critical slowing down at a bifurcation," Am. J. Phys. **72**, 799–809 (2004).
[54] Wechselberger, M., Mitry, J., and Rinzel, J., "Canard theory and excitability," in *Nonautonomous Dynamical Systems in the Life Sciences*, edited by P. E. Kloeden and C. Pötzsche (Springer International Publishing, 2013) pp. 89–132.
[55] Wieczorek, S., Ashwin, P., Luke, C. M., and Cox, P. M., "Excitability in ramped systems: the compost-bomb instability," Proceedings of the Royal Society A: Mathematical, Physical and Engineering Sciences **467**, 1243–1269 (2011).
[56] Wieczorek, S., Xie, C., and Ashwin, P., "Rate-induced tipping: thresholds, edge states and connecting orbits," Nonlinearity **36**, 3238–3293 (2023).
[57] Wieczorek, S., Xie, C., and Jones, C. K. R. T., "Compactification for asymptotically autonomous dynamical systems: theory, applications and invariant manifolds," Nonlinearity **34**, 2970 (2021).
[58] Wilson, T. A.and Beavers, G. S., "Operating modes of the clarinet," J. Acoust. Soc. Am. **56**, 653–658 (1974).
[59] Wolfram Research, Inc.,, "Mathematica, Version 13.2," Champaign, IL, 2022.